



Simulation of a shut-down transient in the Francis-99 turbine model

Downloaded from: <https://research.chalmers.se>, 2023-05-04 18:42 UTC

Citation for the original published paper (version of record):

Uppström, L., Fahlbeck, J., Lillberg, E. et al (2019). Simulation of a shut-down transient in the Francis-99 turbine model. IOP Conference Series: Earth and Environmental Science, 405(1).
<http://dx.doi.org/10.1088/1755-1315/405/1/012026>

N.B. When citing this work, cite the original published paper.

Simulation of a shut-down transient in the Francis-99 turbine model

L Uppström¹, J Fahlbeck¹, E Lillberg² and H Nilsson¹

¹ Chalmers University of Technology, Mechanics and Maritime Sciences, Sweden

² Vattenfall AB Research and Development, Sweden

Corresponding author: hakan.nilsson@chalmers.se

Keywords: Transients, Rotor-stator interaction, Mesh morphing, Hydropower

Abstract. Due to the new intermittent electric energy sources, hydropower is forced to run more and more at off-design conditions and to regulate the operating conditions. This causes flow instabilities with pressure fluctuations, and load variations that may deteriorate the machine. Previous numerical research on the flow in water turbines has mainly focused on steady operating conditions at BEP and off-design. More knowledge is needed on transients between operating conditions, and start-up and shut-down procedures. This requires dynamic meshes that both rotate the runner, using a coupling interface to the non-rotating part of the mesh, and morph the guide vane mesh due to the change in guide vane angle during the transient. Special care needs to be taken to apply boundary conditions that resemble the experimental condition to be used for validation. The present work addresses a shut-down transient of the Francis-99 turbine (<https://www.ntnu.edu/nvks/francis-99>), using OpenFOAM-2.3.x. Turbulence is modelled by LES based on the dynamic one-equation eddy viscosity sub-grid model and the cube root volume filter width, although the temporal and spatial resolution requirements have not been assessed in these preliminary results. The inlet and outlet boundary conditions are set using pressure conditions. The outlet static pressure is taken from the experiment at BEP. The inlet total pressure is adjusted to yield the same flow rate as in the experiment at BEP. The flow rate is given by the solution. The runner region of the mesh rotates with a solid-body rotation, while the guide vane region of the mesh is morphing due to the continuous change in guide vane angle. Rotating and stationary parts of the mesh are coupled with an arbitrary mesh interface (AMI). The results show that the methodology can be used to capture the experimentally observed flow features during transients.

1. Introduction

Due to the new intermittent electric energy sources, such as solar and wind, hydropower is forced to run more and more at off-design conditions and to regulate the operating conditions. This causes flow instabilities with pressure fluctuations, and load variations that may deteriorate the machine. One effort to learn more about the flow in water turbines during transients is the Francis-99 workshops, organized at NTNU (<https://www.ntnu.edu/nvks/francis-99>). It is a series of three workshops, where geometrical and experimental data of a Francis turbine model is openly available for validation of CFD results. The first workshop was organized 2014, focusing on three steady operating conditions; the best efficiency point (BEP), a part load point and a high load point. The 14 papers presented at the first workshop [1] showed state-of-the art simulations of the three steady operating conditions using a wide range of CFD codes. The second workshop was organized in 2016 and had a focus on transients between operating conditions. Most of the 10 papers presented at the workshop [2] did however not



investigate the full experimental transients that were made available. The advanced investigations require dynamic meshes that both rotate the runner, using a coupling interface to the non-rotating part of the mesh, and morph the guide vane mesh due to the change in guide vane angle during the transient. Most codes and workshop participants were not ready for such simulations at the time of the workshop. The third workshop was recently organized, but the proceedings are at the time of writing not yet published. It had a focus on FSI of an isolated hydrofoil, as well as isolated stress and strain analysis of the Francis-99 runner.

The present work addresses the scope of the second Francis-99 workshop, using OpenFOAM-2.3.x. The standard code has a class for dynamic mesh motion that can handle rotating regions coupled to stationary regions using the AMI interface. It also has a class for mesh morphing. Those two classes are combined in the present work, to allow simulations with both a rotating runner region and guide vanes that continuously change angle. Due to the large deformation of the guide vane mesh it is necessary to map the fields to new meshes of better quality several times during the procedure.

2. The Francis-99 model turbine test case

The Francis-99 turbine is a 1:5.1 scale model of a prototype Francis turbine located at Tokke power plant, Norway. The model turbine has a net head of about 12m, running at a BEP flow rate of $0.1996\text{m}^3/\text{s}$, and it has a runner diameter of 0.349m. The turbine contains 14 stay vanes, 28 guide vanes and 30 runner blades divided into 15 splitters and 15 full blades. Figure 1 shows the geometry and the locations of the experimental measurements [3]. A number of pressure transducers are mounted at different locations, named VL01 (Vane-Less space), VL2 (not shown in figure 1, but at a similar location as VL01), P42, P71 (Pressure side of runner blade), S51 (Suction side of runner blade), DT11 and DT21 (Draft Tube). DT5 and DT6 are located at similar positions as DT11 and DT21, but at different angles. It should particularly be noted that it is only the experimental data for the pressure at VL2, DT5 and DT6 that is obtained from the second workshop. The other pressure data is from the first workshop, at a slightly different operating condition. PIV measurements of the velocity distribution were made at the plane that is shown as a striped rectangle below the runner, at an angle shown with respect to the spiral casing (top view of spiral casing). Velocity distributions were extracted from the PIV data along Lines 1-3, to the extent of the PIV plane. The experimental data included a shut-down transient from BEP (9.84°) to almost closed guide vanes (0.80°) in 7s, with a constant runner rotational speed of 333 rpm and a constant net head of 12m. This is the transient studied in the present work.

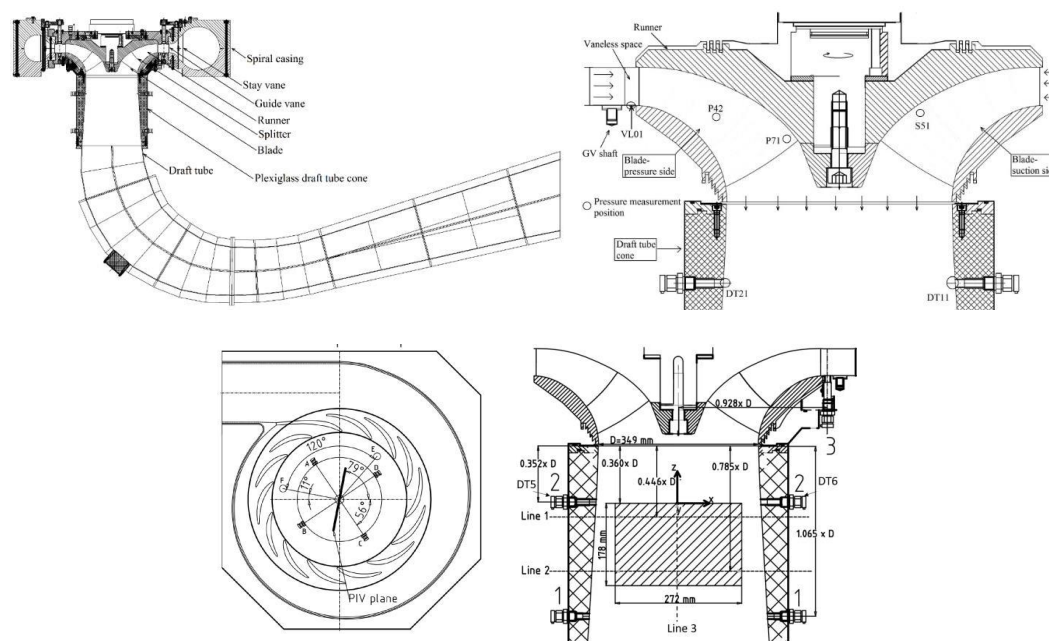


Figure 1. Geometry and locations of experimental measurements.

3. Numerical methods

The simulation of the experimental shut-down transient described in section 2 is performed with OpenFOAM 2.3.x, applying LES with the dynamic one-equation eddy viscosity model, with the cube root volume filter width [4]. It should be noted that the temporal and spatial resolution requirements for LES have not been assessed in this preliminary work that primarily developed and tested features for mesh morphing/motion, rotor-stator-interaction, and inlet/outlet boundary conditions. The time term is discretized with the Crank Nicholson scheme with value 0.5, which in OpenFOAM introduces some stabilizing damping from the Euler scheme. The convection scheme for velocity is 2nd order linear upwind. The large change in guide vane angle deteriorates the mesh, and re-meshing and mapping results is necessary. When switching meshes the Euler and upwind schemes are used for a few first iterations, and the time step is reduced and ramped up again to improve stability. Mean and maximum Courant numbers are 10^{-2} and 30-50, respectively. Pressure boundary conditions are applied to both inlet and outlet, where the outlet static pressure is taken from the experiment at BEP and the inlet total pressure is adjusted to yield the same flow rate as in the experiment at BEP. The inlet and outlet velocities are given by the conservative fluxes, as part of the solution. This enables the conditions to vary during the transient due to the decreasing volume flow rate, as in the experiment.

OpenFOAM 2.3.x provides separate classes for solid-body turbomachinery mesh rotation and morphing meshes. These have been combined in the present work. The guide vane mesh morphing is accomplished via Laplacian smoothing, where the motion imposed by the guide vane boundaries is spread out in the mesh via a diffusivity parameter. Points close to the moving wall are more effected than those further away. The mesh morphing allows to spread into the stay vane region, but not into the runner region. Figure 2 shows a top view of the guide vane mesh during the close-down transient from BEP to almost closed. The BEP mesh, at 9.84° , can be morphed to 6.67° before the mesh quality starts to become inadequate. Then it is necessary to generate a new mesh and map the fields to the new mesh in order to be able to continue the simulation. The new mesh is generated for 4.67° and morphed backward to 6.67° . It is then used for the range 6.67° - 3.68° . The backward morphing reduces the number of needed mesh switches. Additional meshes are generated at 2.0° and 0.8° , which are used in the ranges 3.68° - 1.47° and 1.47° - 0.80° , respectively. All the meshes are generated with cfMesh except for the 0.8° mesh that had to be generated with snappyHexMesh due to the small distance between the guide vanes.

The coupling between the rotating runner mesh and the upstream and downstream guide vane and draft tube mesh regions is achieved using an Arbitrary Mesh Interface (AMI). In the lower part of each of the pictures in figure 2 it is possible to see a top view of the rotating runner mesh and the rotor-stator interface. The total number of cells is 20M, of which 9.36 are in the runner and about 5 are in the guide vane passage.

4. Results

The fully developed results at BEP were validated [5] and used as initial condition for the transient. Due to the pressure boundary conditions applied at the inlet and outlet, the flow rate is given by the simulation. Thus, the inlet total pressure was adjusted to yield the correct flow rate at BEP before starting the simulation of the transient. The volumetric flow rates are 0.1996 m³/s and 0.1965 m³/s for experiment and simulation before the closing commences, a difference of 1.55 %. The flow rates after shutdown are 0.0220 m³/s and 0.0168 m³/s, which corresponds to a difference of 23.6 %, i.e. the deviation has increased but this is for very small absolute values. Hence it is verified that the pressure boundary condition works as intended.

Figure 3 shows the experimental and numerical static pressure development at VL2, DT5 and DT6, as the guide vanes start closing at $t=1$ s (at 9.84°) and change angle linearly during 7s (to 0.8° , where 0° is fully closed). The experimental data at DT5 and DT6 was presented as deviation from the mean value of each sequence, as then also done for the numerical data. It can be seen that both the general trend and the magnitude of the pressure fluctuations are similar. The major peaks in the numerical results are due to the switches between meshes.

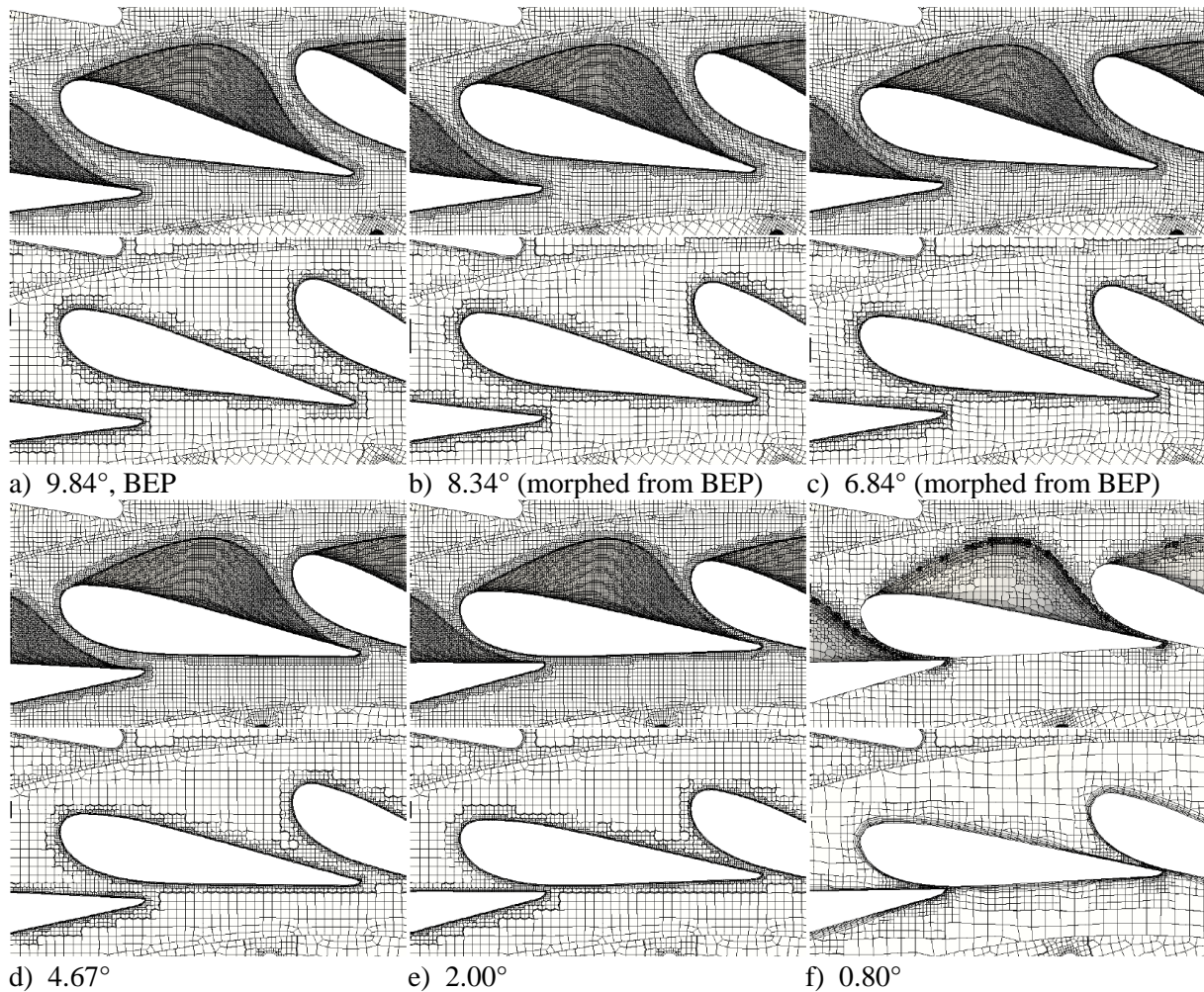


Figure 2. Guide vane meshes during close-down transient. Top: At upper cover (also showing a part of the special shape of the guide vane walls, at the densely meshed region above the guide vane). Bottom: Mid-plane. Angles are from fully closed position.

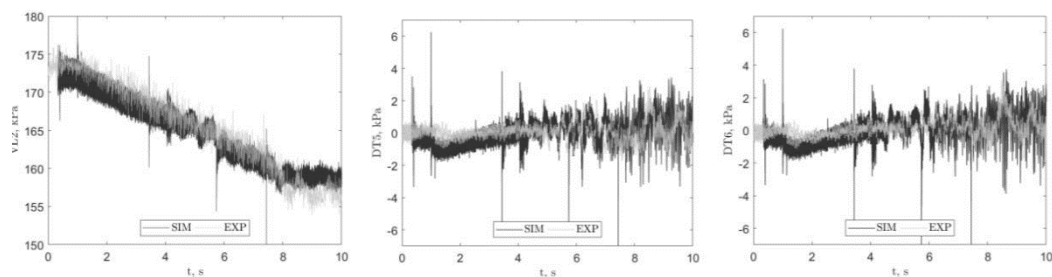


Figure 3. Transient experimental (EXP) and numerical (SIM) static pressure comparison at probes VL2 (left), DT5 (center), and DT6 (right), going from BEP and closing the guide vanes linearly from $t=1$ s to $t=8$ s.

Figure 4 shows contour plots of the velocity along Lines 1 and 2 during the shutdown transient. The r/R_{\max} -axis is along the measurement lines, and the t -axis is along the time (bottom to top). Both the experimental and numerical data is probed at 28 positions along the r/R_{\max} -axis. The numerical data has been filtered using a filter width of 15 (using 7 time steps before and after the corresponding time step), and is presented every 50 time step to reduce the influence of the instantaneous turbulent fields. The experimental procedure must involve smoothing both in time and space, but it has not been described in detail in the Francis-99 workshop instructions. The general trends are captured over the

entire line, but the simulations shows more diffusive transitions between different regions. A tendency to generate larger turbulent structures is produced by the simulation.

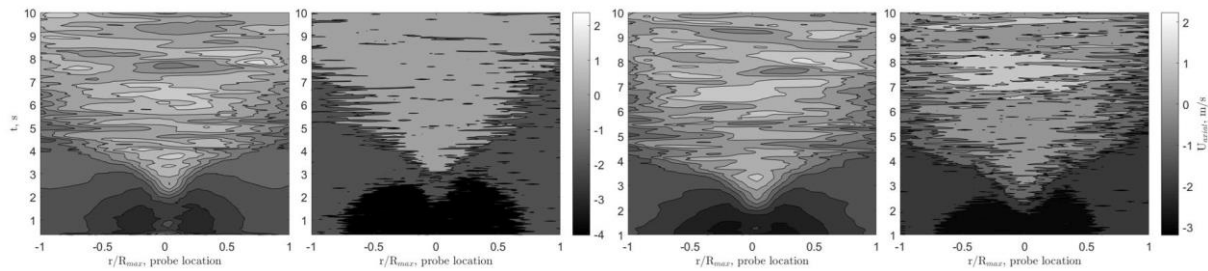


Figure 4. Velocity along line 1 (left pair) and line 2 (right pair) over time (vertical axis). In each pair, Left: simulation. Right: experiment. The guide vanes close linearly from $t=1$ s to $t=8$ s.

The time-history of the axial and horizontal velocities in point 10 of 28 along line 1 can be seen in figure 5. The general behaviour is very similar between the numerical and experimental data, with stronger fluctuations at the same phase of the shut-down transient. This indicates a build-up of a flow-induced instability. The rapid axial deceleration of the flow between 1.5-4.5s ($\alpha=9.2^\circ$ - 5.3°) due to the closing guide vanes is nicely captured. Similar behaviour is also observed at line 2, with even better agreement between numerical and experimental results.

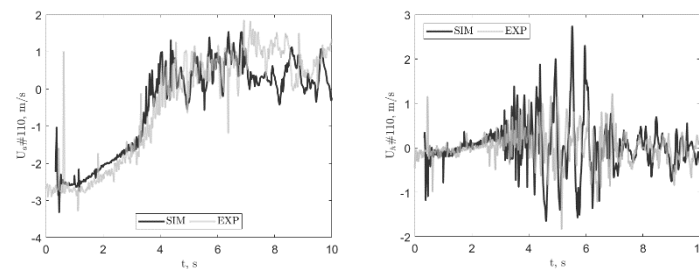


Figure 5. Axial (left) and horizontal (right) velocity during shutdown for velocity line 1, at point 10 of 28.

Figure 6 shows the numerical runner torque during shut-down, filtered with a width of three. The axial torque decreases linearly to almost zero Nm. The torque around x and y are comparably small, as they should be in a well-designed machine. However, large unsteady behaviours in M_x and M_y are observed from $t \approx 4$ -6.5s. These times correlate well with the unsteadiness seen for the horizontal velocity components in figure 5, right after the fast deceleration of axial velocity. The abrupt changes in M_x and M_y , although being small, would subject the shaft bearings to unwanted fatigue loads, which might deteriorate them and thus the entire machine.

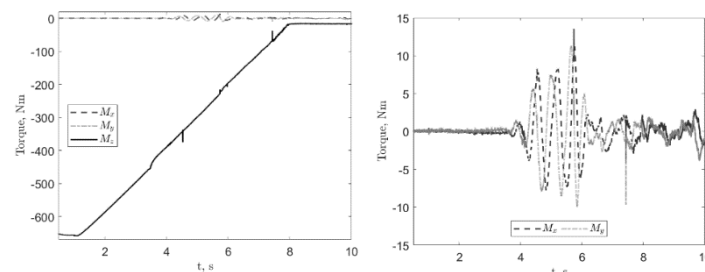


Figure 6. Torque along the x, y and z axes. Left: All components. Right: x and y components.

When looking at the central vortex rope using the Q-criterion one can see a significant change in flow behaviour during the transient, see figure 7. The initial small central vortex indicates a relatively stable flow with a high axial and a moderate tangential velocity. As the velocity decreases, the flow is diverging towards the wall and the tangential velocity becomes dominant. This creates a wider vortex

in the center of the draft tube that eventually breaks up in 2-3 processing vortices, which finally breaks up in several more chaotic vortices.

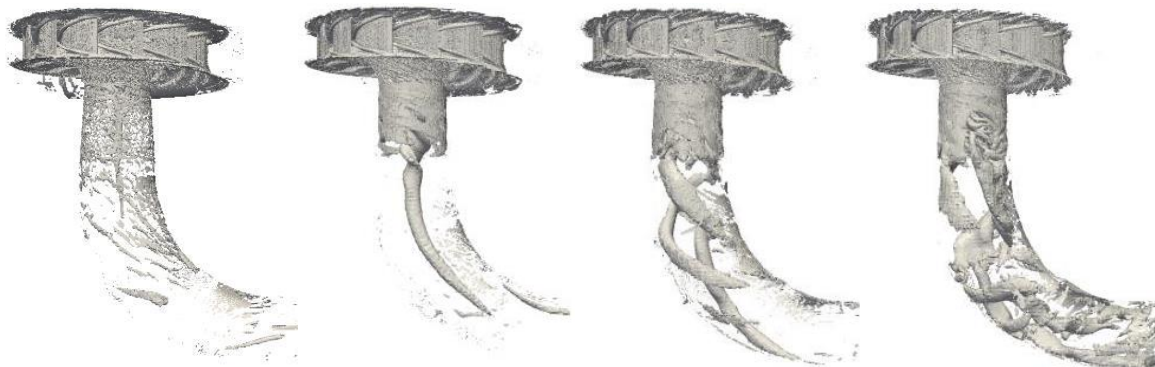


Figure 7. Iso-surface of the Q-criterion (iso-value 200), showing the change in large-scale structures during the transient. Left: BEP, at initiation of guide vane closing. Center left: guide vanes appr. 3.3° from BEP. Center right: guide vanes appr. 4.2° from BEP. Right: guide vanes appr. 6.2° from BEP.

5. Conclusions

A combination of rotating and morphing mesh regions has been proven reliable to simulate the shutdown transient. Both pressure and velocities are compared with experimental values and the general behaviour is coinciding to a satisfying extend in most cases.

A pulsating behaviour is encountered for guide vane angle range $5.9\text{--}2.7^\circ$ (4–6.5s), in several plots. It plausibly originates from the destruction of the vortex rope. This gives rise to fluctuations in the non-axial torque, which may contribute to deterioration of the machine.

Further work is needed with respect to many aspects, e.g.: The mesh morphing procedure is too complicated and involves time-consuming hands-on work. The implementation of combined morphing and rotation needs to be more general and robust. The switching between meshes due to the large mesh deformation gives peaks that should be addressed. The inlet and outlet boundary conditions need to be further addressed in order to better correspond to the conditions during transients. The temporal and spatial resolution requirements of the turbulence model need to be addressed once the practical issues are resolved, to get accurate results. The high Reynolds number may force the use of hybrid models.

Acknowledgements

The authors thank the Swedish Hydropower Centre for financial support.

References

- [1] Cervantes M, Trivedi C, Dahlhaug O G and Nielsen T K (editors) 2015 Francis-99 workshop 1: steady operation of Francis turbines, *IOP Conf. Series: Journal of Physics: Conf. Series* 579 (2015) 011001, doi:10.1088/1742-6596/579/1/011001
- [2] Cervantes M, Trivedi C, Dahlhaug O G and Nielsen T K (editors) 2017 Francis-99 Workshop 2: transient operation of Francis turbines *IOP Conf. Series: Journal of Physics: Conf. Series* 782 (2017) 011001, doi:10.1088/1742-6596/782/1/011001
- [3] Trivedi C, Cervantes M and Dahlhaug OG 2016 Experimental and Numerical Studies of a High-Head Francis Turbine: A Review of the Francis-99 Test Case *Energies*, vol. 9/no. 2, pp. 1-24.
- [4] Lillberg E and Nilsson P 2008 Generic CFD for Vortex Induced Acoustic Resonance in Deep Cavities *ICONE16*
- [5] Fahlbeck J and Uppström L 2018 LES of transients in the Francis-99 turbine *Master's thesis 2018:17*, Department of mechanics and maritime sciences, Chalmers university of technology.